

# Assessing the acid strength of solid acid catalysts with the use of linear free energy relationship: H/D exchange with substituted benzene derivatives

Valter L.C. Gonçalves, Rogério C. Rodrigues, Rodolfo Lorençato, Claudio J.A. Mota \*

Universidade Federal do Rio de Janeiro, Instituto de Química, Av. Athos da Silveira Ramos 149, Cidade Universitária CT Bl A, 21941-909 Rio de Janeiro, Brazil

Received 31 October 2006; revised 14 February 2007; accepted 8 March 2007

Available online 20 April 2007

## Abstract

The acid strength of solid acid materials can be assessed using the linear free energy relationship, applying the Hammett–Brown equation ( $\log k_X/k_H = \rho\sigma^+$ ) for the H/D exchange with substituted benzenes. The magnitude of the  $\rho$  varies for different solid acid materials (Amberlyst-15, zeolite HUSY, K-10 montmorillonite, and niobic acid) and is associated with the degree of proton transfer in the transition state. The results were compared with the  $\rho$  values obtained for H/D exchange with sulfuric acid solutions, indicating that neither solid acid is stronger than 98% sulfuric acid solution. Calculations also revealed that H/D exchange is mostly concerted, with little degree of charge development in the aromatic ring in the transition state.

© 2007 Elsevier Inc. All rights reserved.

**Keywords:** Acidity; Zeolites; Solid acids; Linear free energy; H/D exchange

## 1. Introduction

There is a broad spectrum of reported acid strength for solid acids like zeolites, mixed oxides, and clays, each one depending on the method used [1–3]. The presence of metals, cations, and confinement effects makes the quantitative description of proton transfer on solid acids a difficult task. For zeolites, the situation is even more complex. Although the crystalline structure and presence of extra-framework alumina (EFAL) have a significant influence on catalytic properties [4], studies have shown that the acid strength is similar regardless of the zeolite structure [5] and the presence of EFAL species [6], suggesting that other effects may play a role in governing the catalytic activity. In this study, we show that the linear free energy relationship (LFER) for the H/D exchange of substituted benzenes can be used to help evaluate the acid strength of solid acid materials and correlate this value with the acidity of sulfuric acid solutions.

The LFER is used to quantify the electronic effects of a substituent in a particular reaction [7]. Hammett used the ionization

constant of substituted benzoic acids in water [8] to assess the  $\sigma$  parameter for each substituent. The main idea is that the ionization constant for the substituted benzoic acid, and consequently the Gibbs free energy variation, is affected by the electronic factors of the substituent and treated as a perturbation of the Gibbs free energy of the benzoic acid. Hence, a LFER was created. For hydrogen,  $\sigma$  is 0 by definition. Electron-withdrawing substituents, such as nitro and cyano, have positive  $\sigma$  values (increasing the ionization constant relative to benzoic acid), whereas electron-releasing substituents, such as methyl and methoxy, have negative  $\sigma$  parameters (decreasing the ionization constant relative to benzoic acid). The  $\sigma$  parameters were tabulated for substituents in para and meta positions, relative to the reaction center, to avoid possible steric interference when considering the ortho position. The  $\sigma$  parameter developed by Hammett does not include resonance effects on the substituent; therefore, Brown [9] introduced a new parameter ( $\sigma^+$ ), from the solvolysis of the substituted cumyl chlorides in aqueous acetone, to account for the resonance of positive charge in the ring during the reaction.

The LFER can be applied to other reactions using the Hammett equation ( $\log k_X/k_H = \rho\sigma$ ) or the Hammett–Brown equation, with  $\sigma^+$  replacing the  $\sigma$  to account for resonance with

\* Corresponding author.

E-mail address: [cmota@iq.ufrj.br](mailto:cmota@iq.ufrj.br) (C.J.A. Mota).

the substituent. They can be useful for measuring the electronic effects on reaction rates or equilibrium. The slope ( $\rho$ ) of a plot of the logarithm of the relative rate ( $k_X/k_H$ ) against the  $\sigma$  or  $\sigma^+$  is associated with the electronic effects on the reaction rate or equilibrium. A positive value means that the electron-withdrawing substituent favors the reaction, whereas a negative value means the opposite. The larger the electronic effect, the greater the magnitude of the slope, which permits comparison of different chemical systems. The  $\rho$  value represents the sensitivity of the reaction to electron withdrawal and donation compared with benzoic acid ionization, which, by definition, has a  $\rho$  of 1.0. Jaffé [10] reviewed the application of LFER to several chemical systems and tabulated the respective  $\rho$  values.

There have been few applications of LFER to heterogeneous catalysis. Mochida and Yoneda [11–14] reported a series of studies related to dealkylation, isomerization, and cracking of hydrocarbons, correlating the rate with the enthalpy of hydride abstraction. Franklin and Nicholson [15] have also reported correlation of the activation energy for hydrocarbon cracking on silica-alumina, with the ionization potential of the hydrocarbon. Ramirez-Corredores et al. [16] correlated experimental reactivity data for hydrodesulfurization with the calculated energy parameters of different metal-sulfide catalysts. Finiels et al. [17] reported an interesting survey of LFER studies, using the Hammett equation, for metal, sulfide, and acid catalysts. They reported a  $\rho$  of +0.4 for the hydrogenation of halonitrobenzenes over conventional NiMo and CoMo catalysts, whereas a value of +0.7 was found over Pt/Al<sub>2</sub>O<sub>3</sub> catalyst, indicating a similar mechanism on both catalysts. Moreau et al. [18] found similarities between homogeneous and heterogeneous acid-catalyzed hydrolysis of acetals. In solution, the observed  $\rho$  is  $-3.3$ , whereas in K-10 montmorillonite and mordenite catalysts, these values are  $-2.7$  and  $-3.2$ , respectively.

The H/D exchange of solid acids with alkanes for studying the mechanism of protonation and the formation of carbocations on solid surfaces has been reported in the literature [19–24]. Baumgarten and Zachos [25] reported the H/D ex-

change of benzene with chlorinated alumina catalysts, showing that the Bronsted acid sites are stronger in these catalysts than in pure Al<sub>2</sub>O<sub>3</sub>, as observed by the lower activation energy. Gorte et al. [26] reported that H/D exchange of DZSM-5 with toluene occurs exclusively at the ortho and para positions, similar to what occurs in solution. Haw et al. [27] reported an experimental and theoretical H/D exchange of benzene with zeolite catalysts and found activation energies of 14.4 kcal/mol for ZSM-5 and 20.3 kcal/mol for USY zeolite. This latter result is in good agreement with calculated activation energy using a T<sub>3</sub> cluster model and DFT-level theory, which also indicated that the transition state is highly symmetric, consistent with a concerted process.

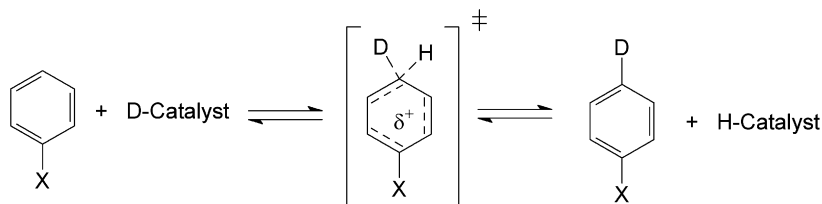
Here we used the H/D exchange between substituted benzenes and solid acid materials to assess the degree of proton transfer, as pictured in Scheme 1. The basic hypothesis of this work is that stronger acid materials will lead to a more polar transition state with an increased degree of proton transfer to the aromatic, being more affected by the electronic effects of the substituent. This will be reflected in the magnitude of the slope ( $\rho$ ), which will be larger in modulus. In addition, we compared the results with sulfuric acid solutions and *n*-butylamine thermo-desorption.

## 2. Experimental

### 2.1. Materials

The Amberlyst-15 acid resin was obtained from Hoom and Hass, whereas the K-10 montmorillonite was purchased from Fluka. Niobic acid was supplied by CBMM (Brazilian Company of Metallurgy and Mining) and HUSY by Petrobras. Table 1 gives characterization data and pretreatment temperatures.

The H/D exchange was examined using benzene, toluene, anisole, bromobenzene, chlorobenzene, cyanobenzene, and nitrobenzene over each catalyst. All reactants were purchased with more than 99% purity and subjected to additional standard purification methods [28]. The purity of each aromatic



Scheme 1. H/D exchange of substituted benzene, showing the transition state with charge development in the ring.

Table 1  
Characterization of the catalysts and pre-treatment temperature

Catalyst	Area (m <sup>2</sup> /g)	Si/Al molar ratio	Pre-treatment temperature (°C)
Amberlyst-15	50	–	150
K-10	240	6.6	150
Niobic acid	187	–	350
HUSY	566	2.6 <sup>a</sup> (4.5) <sup>b</sup>	500

<sup>a</sup> Chemical Si/Al ratio, measured by X-ray fluorescence.

<sup>b</sup> Framework Si/Al ratio, measured by infrared.

was checked by gas chromatography coupled with mass spectrometry; all were 99.5–99.8% pure. Deuterated water (99.9%), 98% D<sub>2</sub>SO<sub>4</sub>, and *n*-butylamine were purchased from Aldrich and used without purification.

## 2.2. *n*-Butylamine titration

The acid strength distribution of all catalysts except Amberlyst-15 (which does not have great thermal stability) was measured by *n*-butylamine thermo-desorption, using thermogravimetric experiments to monitor the weight loss. About 25 mg of catalyst was initially pretreated in a straight glass reactor, under flowing helium (40 mL/min), to the temperatures given in Table 1. The temperature was subsequently set to 150 °C, and the flow of helium (10 mL/min) was driven to a saturator containing *n*-butylamine at room temperature. The flow of *n*-butylamine over the catalyst was maintained for 10 min, and the excess amine was desorbed by passing a flow of helium (20 mL/min) over the catalyst bed for 20 min. The solid was then carefully placed in the thermogravimetric equipment (Shimadzu TGA-51), and the TPD profile was obtained after the weight loss, under flowing nitrogen gas.

## 2.3. H/D exchange measurement (flow conditions)

First, the catalyst (about 200 mg) was pretreated under a flow (40 mL/min) of dry nitrogen gas. Then, the catalyst was deuterated by directing the flow of nitrogen to a saturator containing deuterated water. The H/D exchange was carried out at 100 °C by injecting an equimolar mixture of benzene and a substituted benzene (anisole, toluene, bromobenzene, chlorobenzene, cyanobenzene, or nitrobenzene) in the N<sub>2</sub> flow (about 3 mmol of each aromatic hydrocarbon) and collecting the mixture at the reactor outlet for analysis by gas chromatography coupled to a quadrupole mass spectrometer operating in electron impact ionization (70 eV). The degree of deuteration, used to assess the relative rates of H/D exchange, was determined from the *M* + 1 peak after correction for the naturally abundant <sup>13</sup>C contribution, using the selective ion monitoring (SIM) method.

## 2.4. H/D exchange measurement (batch conditions)

The following procedure was used to determine the rate of the H/D exchange with D<sub>2</sub>SO<sub>4</sub> solutions and for USY zeolite at 25 °C to obtain the LFER results. The 60 and 80% D<sub>2</sub>SO<sub>4</sub> solutions were prepared by carefully adding the respective amount

of D<sub>2</sub>O to the 98% D<sub>2</sub>SO<sub>4</sub> solution at low temperature. The exchange experiments were performed mixing the D<sub>2</sub>SO<sub>4</sub> solution with an equimolar mixture of the aromatics under vigorous agitation. The kinetics of H/D exchange were measured by withdrawing samples of the organic layer at specific times.

For the H/D exchange with USY at batch conditions and 25 °C, we initially pretreated and deuterated the catalyst as in the flow condition experiments. The deuterated samples were then transferred to a flask, and an equimolar mixture of the aromatics, dissolved in *n*-hexane, was introduced. The kinetics of H/D exchange were measured by withdrawing samples of the organic layer at specific times.

## 3. Results and discussion

Table 2 shows the results of acid strength distribution obtained with *n*-butylamine thermo-desorption, and Fig. 1 shows the plot for zeolite HUSY. We can see that HUSY is the strongest solid acid material tested by this method, presenting the highest distribution of strong acid sites (350–500 °C), as well as the highest temperature of the associated weight loss derivative, which gives an indication of the average strength of the acid sites at 350–500 °C. Niobic acid, although presenting a lower distribution of acid sites at 350–500 °C, showed a higher temperature of the associated weight loss derivative compared with K-10 montmorillonite, indicating that although there are a lower number of acid sites in the 350–500 °C range, most of these sites are stronger than the sites in K-10 montmorillonite clay catalyst.

Table 3 shows the results of H/D exchange with substituted benzenes for all of the catalysts using  $\sigma$  and  $\sigma^+$  parameters. As usual in this type of plot for electrophilic reactions, the slope ( $\rho$ ) is negative, indicating that electron-withdrawing groups decrease the rate compared with benzene. Amberlyst-15 shows the highest magnitude of the  $\rho$  value among the solids tested, and K-10 montmorillonite shows the lowest. The results indicate that the transition state for H/D exchange with Amberlyst-15 is the most polar, with the highest degree of proton transfer to the aromatic ring. The HUSY zeolite shows  $\rho$  values of  $-1.3$  ( $\sigma$ ) and  $-1.1$  ( $\sigma^+$ ), which are significantly higher in magnitude than the values found for K-10 clay using the same free energy parameter. These results show that the transition state for proton transfer is more polar on zeolite than on amorphous oxide materials, with more protons transferred to the hydrocarbon for delocalization of the positive charge. It is worth mentioning that varying the flow rate of the carrier gas to 20 mL/min does not significantly change the  $\rho$  value (variation

Table 2  
Acid strength distribution by *n*-butylamine thermo-desorption

Catalysts	Weak acidity (mmol g <sup>-1</sup> ) (150–350 °C)	Medium strong acidity (mmol g <sup>-1</sup> ) (350–500 °C)	Total acidity (mmol g <sup>-1</sup> )	Temperature of the maximum weight loss derivative (°C)
HUSY	0.76	1.12	1.88	397
Niobic acid	0.22	0.1	0.32	370
K-10	0.3	0.2	0.5	352

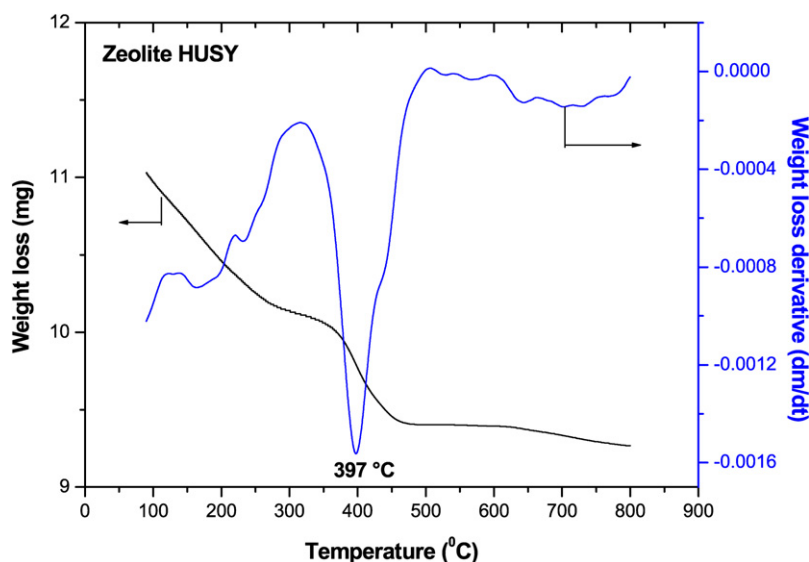


Fig. 1. Plot of *n*-butylamine thermo-desorption on HUSY, showing the weight loss derivative.

Table 3

Linear free energy relationship for the H/D exchange of substituted benzenes with solid acids at 100 °C

Acid system	$\rho(\sigma)$	$(r^2)$	$\rho(\sigma^+)$	$(r^2)$
Amberlyst-15 <sup>a</sup>	-1.7	0.983	-1.3	0.999
HUSY zeolite <sup>b</sup>	-1.3	0.975	-1.1	0.999
HUSY zeolite <sup>c</sup>	-0.5	0.948	-0.3	0.995
Nb <sub>2</sub> O <sub>5</sub> <sup>d</sup>	-0.9	0.982	-0.7	0.998
K-10 montmorillonite <sup>e</sup>	-0.6	0.974	-0.5	0.999
D <sub>2</sub> SO <sub>4</sub> (98%) <sup>f</sup>	-2.0	0.989	-1.5	0.980
D <sub>2</sub> SO <sub>4</sub> (80%) <sup>f</sup>	-1.0	0.987	-0.75	0.984
D <sub>2</sub> SO <sub>4</sub> (60%) <sup>f</sup>	-0.5	0.950	-0.38	0.965

<sup>a</sup> Pre-treated and deuterated at 150 °C.

<sup>b</sup> Pre-treated at 500 °C and deuterated at 200 °C.

<sup>c</sup> Pre-treated at 500 °C and deuterated at 200 °C. Adsorption of *n*-butylamine at 150 °C, followed by heating to 350 °C prior to H/D exchange.

<sup>d</sup> Pre-treated at 350 °C and deuterated at 200 °C.

<sup>e</sup> Pre-treated and deuterated at 150 °C.

<sup>f</sup> Batch experiments at 25 °C. Solutions were prepared by diluting 98% D<sub>2</sub>SO<sub>4</sub> with D<sub>2</sub>O.

in the second decimal), indicating that results of deuteration clearly reflect the kinetics rather than the adsorption/desorption equilibrium of the hydrocarbons.

The LFER results in Table 3 are in agreement with the results of *n*-butylamine thermo-desorption, showing that the  $\rho$  modulus expresses the average acid strength of the material. According to Gorte [1,29], alkylamine thermo-desorption is more suitable than ammonia TPD for assessing the acid strength distribution of Bronsted solid acid materials, especially zeolites. Taking the temperature of the associated weight loss derivative as an indication of the average acid strength in the *n*-butylamine thermo-desorption, we see that the acidity increases in the order K-10 < niobic acid < HUSY. The order is the same if we use the magnitude of the value of  $\rho$ , taken from the H/D exchange measurements, supporting the main idea that a stronger acid site will have a more polar transition state with a higher degree of proton transfer to the hydrocarbon. Unfortunately,

amine thermo-desorption cannot be applied to Amberlyst-15 because of its low thermal stability.

Broad-line <sup>1</sup>H NMR at 4 K has been used to characterize the acidity of many solid acid materials [30]. This method is based on the interaction of water with the acid sites to form H<sub>3</sub>O<sup>+</sup> ions. The acidity coefficient is defined as the number of hydronium ions per Bronsted acid site when adsorbed water interacts with all the Bronsted acid sites [31] and provides a measure of the acid strength of the solid acid material. Sulfuric acid and Nafion sulfonic acid resin have an acidity coefficient of 1 [32,33], indicating that each proton interacts with the water molecule to form the hydronium ion. For zeolites and niobic acid, the situation is different. The acidity coefficients range from 0.2 to 0.4 for zeolite Y [33], depending on dealumination and the presence of EFAL, whereas niobic acid has an acidity coefficient of 0.2 [31,34]. Although there have been no studies on the acidity of Amberlyst-15 with this technique, it is reasonable to believe that the activity coefficient should be similar to that found for Nafion and sulfuric acid, because of the leveling effect of water for sulfonic-based acids [31]. The LFER results of H/D exchange shown in Table 3 are in good agreement with the reported results of acidity coefficients measured by broad-line <sup>1</sup>H NMR at 4 K for water adsorption, indicating that LFER results of H/D exchange of substituted benzenes can also be used to estimate the acid strength of solid acid materials.

To provide additional evidence of the relationship between  $\rho$  and the acid strength of the solid, we first adsorbed *n*-butylamine at 150 °C over deuterated USY zeolite and heated the sample to 350 °C under flowing nitrogen (40 mL/min). Then we carried out the H/D exchange at 100 °C. On base adsorption and heat treatment, most of the acid sites (especially the strongest ones) were neutralized and inactive for H/D exchange. The slope of the line was significantly lower, as shown in Fig. 2 and Table 3. After *n*-butylamine neutralization, the  $\rho$  values were -0.3 ( $\sigma^+$ ) and -0.5 ( $\sigma$ ), considerably lower in magnitude than the -1.1 ( $\sigma^+$ ) and -1.3 ( $\sigma$ ) found for the zeolite HUSY without neutralization. These results clearly show

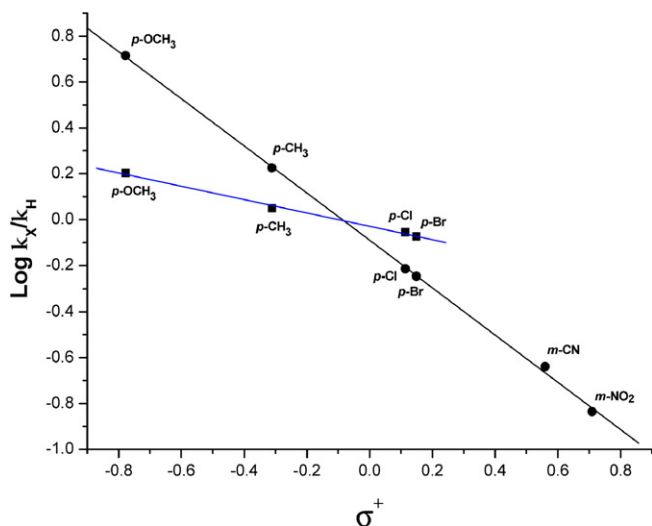


Fig. 2. Linear free energy plot for the H/D exchange with HUSY zeolite. (●) No base adsorption,  $\rho = -1.1$  ( $r^2 = 0.998$ ); (■) adsorption of *n*-butylamine at 150 °C, followed by heating to 350 °C prior to H/D exchange,  $\rho = -0.3$  ( $r^2 = 0.999$ ).

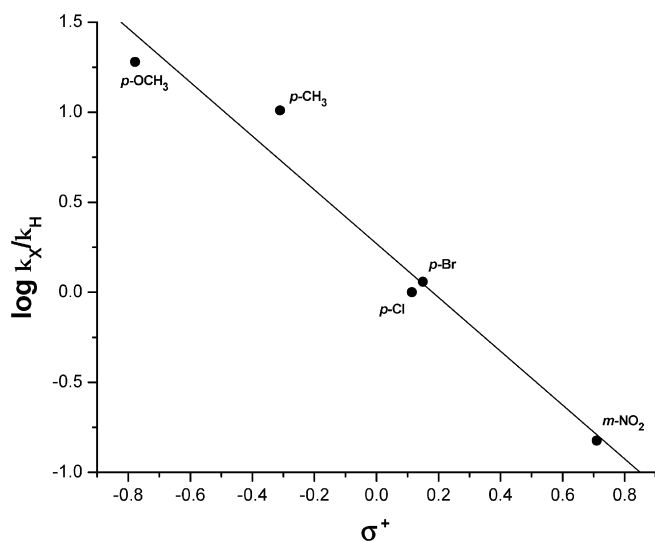


Fig. 3. Linear free energy plot for H/D exchange with D<sub>2</sub>SO<sub>4</sub> 98% at 25 °C ( $\rho = -1.5$  and  $R^2 = 0.98$ ).

that the magnitude of the  $\rho$  is in consonance with the acid strength of the material. On neutralizing the strongest acid sites of the zeolite catalyst, the H/D exchange occurred with a less-polar transition state, indicating that the remaining acid sites show a lower degree of proton transfer to the aromatic hydrocarbon in the transition state.

We also carried out H/D exchange of substituted benzenes with D<sub>2</sub>SO<sub>4</sub> solutions to compare the acid strength of solid and liquid acids. Table 3 gives the results for three different concentrations of D<sub>2</sub>SO<sub>4</sub>, and Fig. 3 gives the LFER plot for 98% D<sub>2</sub>SO<sub>4</sub>, showing the relationship between the magnitude of  $\rho$  and the acid concentration. The strongest solid acids tested—Amberlyst-15 and HUSY zeolite—are weaker than 98% sulfuric acid but stronger than 80% sulfuric acid solution. On the other hand, K-10 montmorillonite and niobic acid have acid-

ity within 60–80% sulfuric acid solutions. To check the effect of temperature, we carried out H/D exchange with USY zeolite at 25 °C under batch conditions, using *n*-hexane as solvent. The measured  $\rho(\sigma^+)$  differed in the second decimal from the value obtained at 100 °C under flow conditions. This result indicates that temperature has little effect, as expected from the values of  $\rho$  (near unit), indicating minor changes in activation energy as a function of the substituent. Therefore, the  $\rho$  value obtained for solid acids can be associated with a respective sulfuric acid solution and, consequently, with the Hammett acid function (Ho). For instance, the Ho of 98% sulfuric acid solution is  $-10.44$ , whereas those for the 80 and 60% solutions are  $-7.34$  and  $-4.46$ , respectively. Although neither of the solid acids tested specifically matched these sulfuric acid concentrations, it is possible to search for a concentration of D<sub>2</sub>SO<sub>4</sub> with a value of  $\rho$  closer to that found for the solid acid catalysts and then correlate it with the respective Ho value.

The absolute values of  $\rho$  found for all of the solid materials used in this study are low compared with other electrophilic aromatic substitution reactions. For instance, a LFER study of Friedel–Crafts acylation over zeolite catalyst showed a  $\rho$  of  $-5.0$  [17,35]. Chlorination of aromatic hydrocarbons exhibited a  $\rho$  of  $-8.1$  [9], indicative of a transition state with large degree of charge transfer to the aromatic ring. The magnitude of the  $\rho$  in these reactions reflects the electrophilic nature of the attacking species and how they proceed to the transition state. In acylation, the acyl cation is believed to be the attacking species, whereas in chlorination, a positive chlorine species is normally involved in the reaction mechanism. Both species are highly electrophilic and induce an earlier transition state, demanding electrons from the aromatic ring. This is reflected in the highly negative  $\rho$  values found for these reactions. The observed  $\rho$  for H/D exchange on solid acids is similar in magnitude to the values found for carbene addition reactions [36], which are moderate electrophilic intermediates thought to react through a more concerted transition state with a lower degree of charge separation. The range of  $\rho$  values observed for H/D exchange with solid acids is also similar in magnitude to those found in hydrogen abstraction of substituted toluenes by free radical species. For instance, highly reactive species, such as the bromine atom (Br•), has a  $\rho$  of  $-1.46$  (correlation with  $\sigma^+$ ), which is consistent with a transition state developing positive charge in the aromatic ring [37]. However, the magnitude of  $\rho$  varies as a function of the attacking radical species [38]. The *tert*-butoxy radical has a  $\rho$  of  $-0.34$ , whereas less-reactive radicals, such as phenyl or even the hydrogen atom have a  $\rho$  near 0, indicative of a transition state with very little degree of charge transfer to the aromatic ring. These results reinforce the relationship of  $\rho$  with the degree of charge transfer in the transition state, even for nonionic reactions.

To gain more insight into the meaning of the  $\rho$  value, we carried out quantum mechanical calculations. Fig. 4 shows the calculated transition state for H/H exchange of benzene with zeolite Y, using the ONIOM method implemented in the Gaussian 98 program [39]. The aromatic compound and the active site (T3) were treated at the DFT level of calculation, and the rest of the zeolite structure at the MNDO level. The struc-

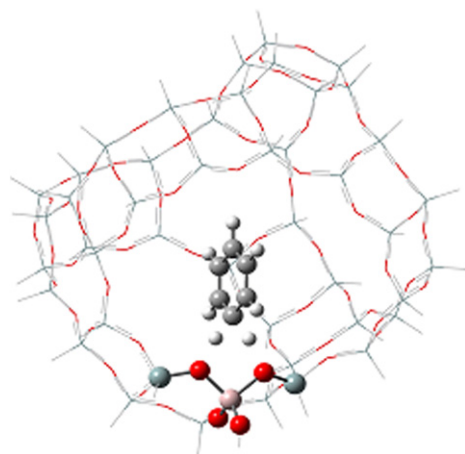


Fig. 4. Calculated transition state for H/H exchange of benzene with zeolite Y, at ONIOM B3LYP/6-31G(*d, p*):MND0 level.

ture presents symmetry, indicating a concerted process. The exchanging C–H bond lengths are 1.195 and 1.212 Å, whereas the O–H bond lengths are 1.50 and 1.54 Å. A charge distribution analysis using the ChelpG scheme [40,41] indicated that, compared with the isolated aromatic molecule, there is little charge development in the ring in the transition state. For benzene, the charge increment in the para carbon atom (relative to the exchanging carbon atom) is +0.05, explaining the low  $\rho$  value found in the experiments. This might explain why the correlation coefficients ( $r^2$ ) for fitting the data with  $\sigma$  or  $\sigma^+$  are close, although the reaction is better described by the  $\sigma^+$  parameter, which accounts for delocalization of the positive charge in the aromatic ring. These calculations are in agreement with other theoretical studies of H/D exchange [18,23,42,43], which indicated a more concerted mechanism.

For all of the acids tested, proton transfer presented a  $\rho$  near unit. This reflects the nature of the electrophilic species in acids, where the proton is covalently bonded to the oxygen atoms. This characteristic leads to a later transition state with a significant degree of coordination of the attacking proton with the oxygen atom of the acid system and, consequently, lower demand of electrons from the aromatic ring. On the other hand, the naked proton is extremely electrophilic. Gas-phase data on the protonation of substituted benzenes allow us to ascertain the  $\rho$  value from the available free energy data [44]. At 327 °C, the  $\rho$  is  $-21.8$  ( $\sigma^+$ ), indicating the strong electrophilic nature of the proton in gas phase, with no solvation and interaction with other atoms. Nonetheless, the magnitude of the  $\rho$  for H/D exchange with substituted benzenes might be associated with the acid strength of the material, as clearly shown by the sulfuric acid solutions and comparisons of the data with other acid-strength methods, especially amine thermo-desorption and broad-line  $^1\text{H}$  NMR results. The solid acids tested differ in the nature of the acid site, as well as in their catalytic properties. Amberlyst-15 is a sulfonic acid resin with acidity associated with  $\text{SO}_3\text{H}$  groups. The acidity of zeolites is due to the formation of Si–OH–Al linkages in the framework. The presence of  $\text{H}_3\text{O}^+$  ions formed on dissociation of water molecules coordinated with the metal atoms present in the structure is normally

responsible for the acidity of K-10 and  $\text{Nb}_2\text{O}_5$ . Therefore, the LFER of H/D exchange with substituted benzenes provides additional information to correlate the structure of the active sites with catalytic activity and acid strength of the solid material.

#### 4. Conclusion

The LFER of H/D exchange of substituted benzenes provides a way to infer the polarity of the transition state for proton transfer to the hydrocarbon. The magnitude of the  $\rho$  expresses the degree of proton transfer in the transition state and is associated with the average acid strength of the material. Neither solid acid tested showed a higher  $\rho$  than that of the 98%  $\text{D}_2\text{SO}_4$  solution; Amberlyst-15 and zeolite USY were within 80 and 98% of sulfuric acid solutions, whereas niobic acid and K-10 montmorillonite were within 60 and 80%.

The absolute  $\rho$  values were close to unit, reflecting the nature of the transition state, at which the proton remains coordinated with the oxygen atom of the acid system. In addition, calculations showed a symmetric transition state for the H/D exchange with benzene, indicating a more concerted mechanism and explaining the low absolute  $\rho$  values found for all acid systems compared with other electrophilic reactions.

#### Acknowledgments

The authors thank PRH-ANP, CNPq/CTPETRO, and FAPERJ for financial support.

#### References

- [1] W.E. Farneth, R.J. Gorte, *Chem. Rev.* 95 (1995) 615.
- [2] B. Umansky, J. Engelhardt, W.K. Hall, *J. Catal.* 177 (1991) 128.
- [3] T.E. Xu, J. Munson, J.F. Haw, *J. Am. Chem. Soc.* 116 (1994) 1962.
- [4] R. Carvajal, P.J. Chu, J.H. Lunsford, *J. Catal.* 125 (1990) 121.
- [5] D.J. Parrillo, R.J. Gorte, *J. Phys. Chem.* 97 (1993) 8786.
- [6] A.I. Biaglow, D.J. Parrillo, G.T. Kokotailo, R.J. Gorte, *J. Catal.* 148 (1994) 213.
- [7] T.H. Lowry, K.S. Richardson, *Theory and Mechanism in Organic Chemistry*, Harper & Row, New York, 1981, chapter 2.
- [8] L.P. Hammett, *J. Am. Chem. Soc.* 59 (1937) 96.
- [9] H.C. Brown, Y. Okamoto, *J. Am. Chem. Soc.* 80 (1958) 4979.
- [10] H.H. Jaffé, *Chem. Rev.* 53 (1953) 191.
- [11] I. Mochida, Y. Yoneda, *J. Catal.* 7 (1967) 386.
- [12] I. Mochida, Y. Yoneda, *J. Catal.* 7 (1967) 393.
- [13] Y. Yoneda, *J. Catal.* 9 (1967) 51.
- [14] H. Matsumoto, J.I. Take, Y. Yoneda, *J. Catal.* 11 (1968) 211.
- [15] J.L. Franklin, D.E. Nicholson, *J. Phys. Chem.* 55 (1956) 59.
- [16] M.M. Ramirez-Corredores, I. Machin, M.E. Grillo, *J. Mol. Catal. A* 151 (2000) 271.
- [17] A. Finiels, P. Geneste, C. Moreau, *J. Mol. Catal. A* 107 (1996) 385.
- [18] C. Moreau, R. Durand, P. Geneste, S. Mseidi, *J. Mol. Catal. A* 112 (1996) 133.
- [19] C.J.A. Mota, R.M. Martins, *J. Chem. Soc. Chem. Commun.* (1991) 171.
- [20] G.J. Kramer, R.A. van Santen, C.A. Emels, A.K. Nowak, *Nature* 363 (1993) 529.
- [21] J. Sommer, M. Hachoumy, F. Garin, D. Barthomeuf, *J. Am. Chem. Soc.* 116 (1994) 5491.
- [22] C.J.A. Mota, J. Sommer, M. Hachoumy, R. Jost, *J. Catal.* 172 (1997) 194.
- [23] A.G. Stepanov, S.S. Arzumanov, M.V. Luzgin, H. Ernst, D. Freude, V.N. Parmon, *J. Catal.* 235 (2005) 221.
- [24] M.J. Truitt, S.S. Toporek, R. Rovira-Truitt, J.L. White, *J. Am. Chem. Soc.* 128 (2006) 1847.
- [25] E. Baumgarten, A. Zachos, *Z. Phys. Chem. Neue Fol.* 130 (1982) 211.

- [26] W.E. Farneth, D.C. Roe, T.J. Gricus Kofke, C.J. Tabak, R.J. Gorte, *Langmuir* 4 (1988) 152.
- [27] L.T. Beck, T. Xu, J.B. Nicholas, J.F. Haw, *J. Am. Chem. Soc.* 117 (1995) 11594.
- [28] W.L.F. Amarego, D.D. Perrin, *Purification of Laboratory Chemicals*, fourth ed., Butterworth, Heinemann, Oxford, 2000.
- [29] R. Gorte, *Catal. Lett.* 62 (1999) 1.
- [30] P. Batamack, C. Doremieux-Morin, R. Vicent, J. Fraissard, *J. Phys. Chem.* 97 (1993) 9779.
- [31] V. Semmer, P. Batamack, C. Doremieux-Morin, J. Fraissard, *Top. Catal.* 6 (1998) 119.
- [32] P. Batamack, J. Fraissard, *Catal. Lett.* 35 (1995) 135.
- [33] L. Heeribout, V. Semmer, P. Batamack, C. Doremieux-Morin, J. Fraissard, *Microporous Mesoporous Mater.* 21 (1998) 565.
- [34] P. Batamack, R. Vicent, J. Fraissard, *Catal. Today* 28 (1996) 31.
- [35] B. Chiche, A. Finiels, C. Gauthier, P. Geneste, *Appl. Catal.* 30 (1987) 365.
- [36] Z. Qu, W. Shi, J. Wang, *J. Org. Chem.* 69 (2004) 217.
- [37] T.H. Fisher, A.W. Meierhoefer, *J. Org. Chem.* 48 (1978) 224.
- [38] W.A. Pryor, T.H. Lin, J.P. Stanley, R.W. Henderson, *J. Am. Chem. Soc.* 95 (1973) 6993.
- [39] M.J. Frisch, G.W. Trucks, H.B. Schlegel, G.E. Scuseria, M.A. Robb, J.R. Cheeseman, V.G. Zakrzewski, J.A. Montgomery Jr., R.E. Stratmann, J.C. Burant, S. Dapprich, J.M. Millam, A.D. Daniels, K.N. Kudin, M.C. Strain, O. Farkas, J. Tomasi, V. Barone, M. Cossi, R. Cammi, B. Mennucci, C. Pomelli, C. Adamo, S. Clifford, J. Ochterski, G.A. Petersson, P.Y. Ayala, Q. Cui, K. Morokuma, D.K. Malick, A.D. Rabuck, K. Raghavachari, J.B. Foresman, J. Cioslowski, J.V. Ortiz, A.G. Baboul, B.B. Stefanov, G. Liu, A. Liashenko, P. Piskorz, I. Komaromi, R. Gomperts, R.L. Martin, D.J. Fox, T. Keith, M.A. Al-Laham, C.Y. Peng, A. Nanayakkara, C. Gonzalez, M. Challacombe, P.M.W. Gill, B. Johnson, W. Chen, M.W. Wong, J.L. Andres, C. Gonzalez, M. Head-Gordon, E.S. Replogle, J.A. Pople, *Gaussian 98, Revision A.7*, Gaussian, Inc., Pittsburgh, PA, 1998.
- [40] L.E. Chirlan, M.M. Francl, *J. Comput. Chem.* 8 (1987) 894.
- [41] C. Breneman, M.K.B. Wiberg, *J. Comput. Chem.* 11 (1990) 361.
- [42] P.M. Esteves, M.A.C. Nascimento, C.J.A. Mota, *J. Phys. Chem. B* 103 (1999) 10417.
- [43] P.M. Esteves, A. Ramirez-Solis, C.J.A. Mota, *J. Phys. Chem. B* 105 (2001) 4331.
- [44] Y.K. Lau, P. Kebarle, *J. Am. Chem. Soc.* 98 (1976) 7452.